ELSEVIER

Physica E 12 (2002) 276–280

PHYSICA E

www.elsevier.com/locate/physe

Electron dispersion relations with negative effective masses in quantum wells grown on the cleaved edge of a superlattice

Z.S. Gribnikov[a,b], R.R. Bashirov[a], H. Eisele[b], V.V. Mitin[a,*], G.I. Haddad[b]

[a] *Department of ECE, Wayne State University, Detroit, MI 48202, USA*
[b] *Department of EECS, University of Michigan, Ann Arbor, MI 48109, USA*

Abstract

Engineered energy-wave-vector dispersion relations of either electrons or holes hold great promise for realizing fundamental oscillators at terahertz frequencies if they contain sections with a negative effective mass (NEM) at appropriate energy levels. However, neither bulk semiconductor materials nor quantum wells or quantum wires exhibit such NEM sections in the dispersion relations at favorable energy levels. Therefore, the novel use of a nanostructure is proposed to create an NEM section of electrons at suitable energy levels. This structure utilizes a heterojunction with a quantum well (QW) channel grown perpendicular to a superlattice. At small values of the wave-vector k, the electron wave function Ψ resides mostly in the QW channel and, as k increases, Ψ extends further into the superlattice. This spread of Ψ induces an NEM section in the energy dispersion relation $E(k)$. Several combinations of suitable material systems are considered.

PACS: 73.21.Cd; 85.35.Be

Keywords: Superlattice; Negative effective mass; Negative differential drift velocity; Anticrossing; Cleaved edge; Overgrowth

1. Introduction

A negative differential drift velocity (NDDV), as caused by the negative-effective-mass (NEM) mechanism, does not originate from any kind of carrier scattering such as the intravalley or intervalley scattering. It is the result of how electrons or holes in an electric field follow their respective energy-wave-vector dispersion relations. Therefore, the NDDV of electrons or holes is free of the disadvantages of the transferred-electron effect as known from Gunn devices and, in principle, it is one of the fastest mechanisms of generating high-frequency oscillations. In addition, it may also be realized in the ballistic regime of two-terminal devices or field-effect transistors (FETs) with ultrashort active regions [1]. Even in the case of dissipative transport, an NDDV leads to oscillations at terahertz frequencies if it is based on the NEM mechanism [2,3].

In most bulk semiconductor materials, however, the NEM mechanism does not exist at energy levels where it can be exploited for high-frequency power generation. An NEM section occurs in the conduction band of practically all well-known semiconductor materials, but at energy levels of typically 0.6–1.0 eV where electron scattering dominates in the transport mechanism. As a result, the NEM mechanism does not play a significant role. For an NEM section to occur at favorable energy levels, two different channels that conduct current and can interact freely must exist. These channels are characterized by substantially

* Corresponding author. Fax: +1-313-577-1101.
E-mail address: mitin@ece6.eng.wayne.edu (V.V. Mitin).

1386-9477/02/$ - see front matter
PII: S1386-9477(01)00372-1

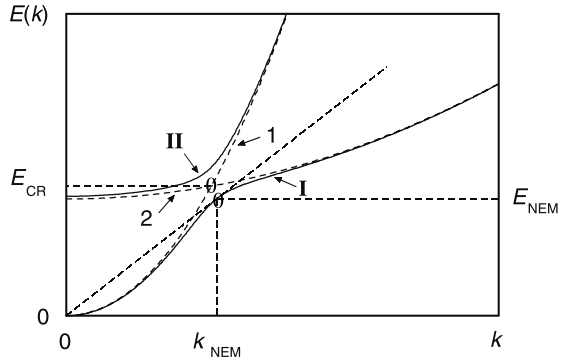

Fig. 1. NEM section in the energy-wave-vector dispersion relation from anti-crossing of the two initial dispersion branches 1 and 2.

different energy dispersion relations, which intersect just at the desired energy level E_{CR} as shown in Fig. 1. This anti-crossing from the interchannel interaction then forms the hybrid dispersion branches I and II, where the lower branch I contains the desired NEM section. The difficulty of implementing this approach lies in selecting two parallel channels 1 and 2 that contain electrons (or holes) with very different effective masses ($m_2 > 2m_1$) at relevant energy levels. Any method of hybridization must avoid the deformation of the original energy dispersion relations as well as the influence of electron (or hole) scattering. Instead, it must provide a substantial interchannel electron (or hole) exchange without collisions.

Such hybridization is known to exist in p-type quantum wells (QWs) and quantum wires where the two conductive channels are formed by the energetically split heavy and light holes. The exchange comes from spin–orbital interaction in the abrupt well and wire sidewalls, but achievable barrier heights of these sidewalls severely limit the energy range of the NEM section. NEM sections also exist in the valence bands of wurtzite semiconductor materials as well as in uniaxially compressed p-type zincblende semiconductor materials. At energy levels of 0.01–0.03 eV, however, such NEM mechanisms based on holes are suitable only for cryogenic temperatures.

2. Discussion

In this paper, the use of a superlattice (SL) as a channel with a high effective electron mass and a heterojunction perpendicular to the SL as a channel with a low effective mass is proposed. The schematic structure of such a system with two parallel channels of very different effective masses is shown in Fig. 2. Electron transport in the SL A–B experiences a very large average effective mass along the z-axis whereas the effective mass in channel C of homogenous material without any SL is very small. The main current carrying channel C is responsible for the initial branch 1 of the dispersion relation in Fig. 1. The SL, which consists of quantum wells ("pockets") A and barrier layers B, is the second parallel channel and, by itself, has the dispersion relation of branch 2. When the energy of electrons in channel C increases in an electric field, their wave functions Ψ penetrate more and more into pockets A. As a result, they become heavier, and their dispersion relation deviates from the initial curve 1 to curve I, which now contains an NEM section. High electron concentration in the two-channel structure is ensured by n-type delta doping in the top barrier layer D. The p-type doping of the SL restricts the electron penetration from channel C of thickness a_C into the pockets of the SL to depth d. The acceptor concentration is chosen such that $d \leqslant (2-4)a_C$.

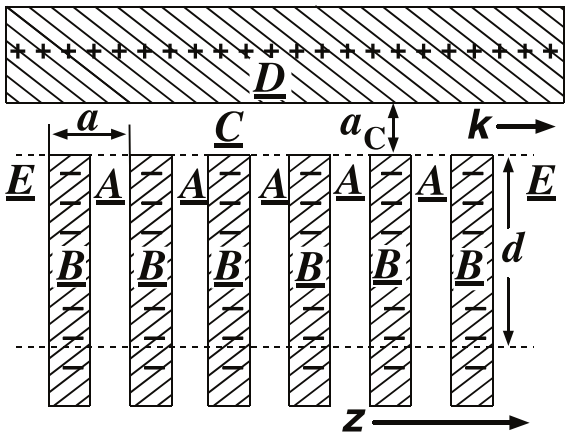

Fig. 2. Schematic of proposed structure with two current carrying channels: main channel C and secondary channel through the superlattice A–B.

The structure of Fig. 2 requires a two-stage in situ epitaxial growth method: First, the SL A–B is grown on a substrate and then the heterojunction C–D on edge E of the SL. Three different approaches to overgrowth on the edge have been reported in the

literature: etching [4,5], cleaving [6], or special methods of epitaxy [7–9] (including molecular beams under a glancing angle [9]). Cleaved-edge overgrowth was demonstrated with the GaAs/AlGaAs and the strained $GaAs/In_xGa_{1-x}As/AlGaAs$ ($x \leqslant 0.25$) material systems [10–12].

A one-dimensional SL period of $a = a_A + a_B$ (a_A = well thickness, a_B = barrier thickness) creates a Brillouin structure in k-space with the period $2\pi/a$ in the direction of the SL (z-axis). For use in a negative-resistance device, the NEM section needs to be in the lowest branch of the dispersion relation and be sufficiently far away from the edge at $k = \pi/a$. First, the so-called initial states are considered separately in channel C and in the SL A–B. The initial branch 1 of the dispersion relation in C, $E_1(k)$, is represented by

$$E_1(k) = E_C(k) \approx E_C(0) + \frac{\hbar^2 k^2}{2m_C}, \quad (1)$$

where $E_C(0)$ is the energy of the quantized ground state at $k = 0$ and m_C is the effective electron mass in channel C, which may be larger than the effective electron mass in the bulk material of C. If the barriers heights of B and D are assumed to be infinite and the quantized electron states in A are assumed to be high as well, the energy $E_C(0)$ can be estimated as

$$E_C(0) = \frac{\hbar^2 \pi^2}{2m_C a_C^2}. \quad (2)$$

For finite barrier heights of B and D and lower levels of the quantized electron states in A, a more realistic value of $E_C(0)$ will be smaller than the one given by Eq. (2).

The dispersion relation of a one-dimensional SL gives the initial branch 2, i.e., $E_2(k)$. For an NEM section to occur at high-energy levels, a large barrier height for B needs to be chosen, which corresponds to a material system with a large conduction band discontinuity δ. In the $GaAs/Al_xGa_{1-x}As$ material system, δ reaches its maximum value of 0.32 eV at $x \approx 0.4$.

Fig. 3(a) shows the energy dispersion relations of the lowest SL miniband for $\delta = 0.32$ eV, $m_A = 0.067m_0$, $m_B = 0.1m_0$ (free-electron mass m_0), and $a = 5.5$ nm. All energy levels are referred to the bottom of the conduction band in bulk GaAs. To find the optimum structure, values of $a = 3.5$, 4, 4.5, 5, and 6 nm were considered. For each value of a, the thickness of B, i.e., a_B, was varied. The resulting variation of the width of the miniband $\Delta(\xi)$ as a function of $\xi = (a_A - a_B)/a$ is plotted in Fig. 3(b) for the same parameters as in Fig. 3(a). It has one minimum at $\xi = \xi_m \approx -0.25$ between the extreme values of $\Delta(\xi = 1) = \hbar^2\pi^2/(2m_A a^2)$ and $\Delta(\xi = -1) = \hbar^2\pi^2/(2m_B a^2)$.

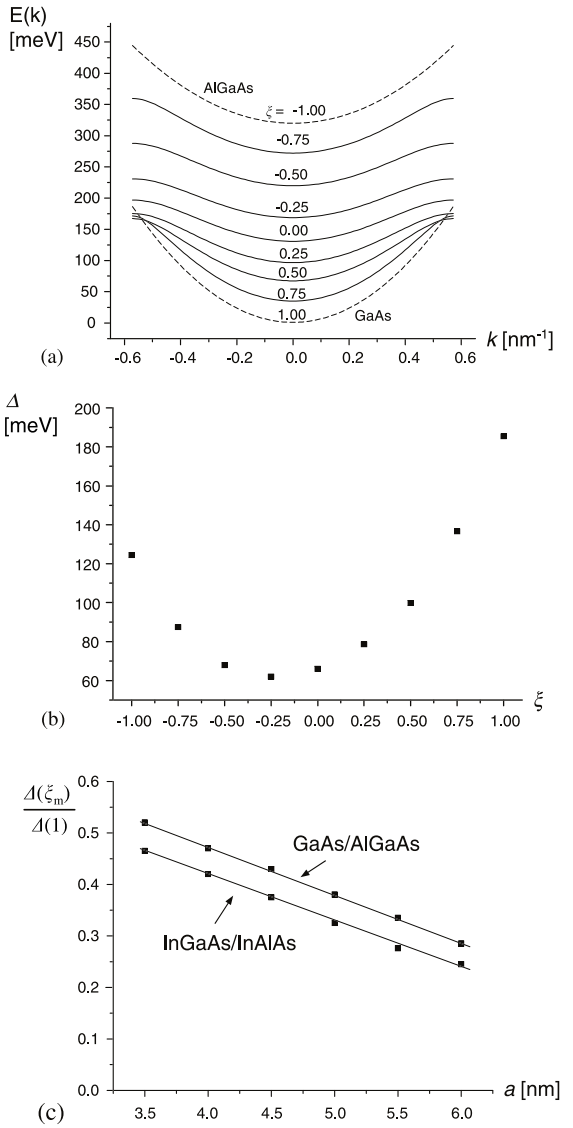

Fig. 3. (a) Miniband dispersion relations of $GaAs/Al_{0.4}Ga_{0.6}As$ superlattices with a period $a = 5.5$ nm for $\xi = (a_A - a_B)/a$; (b) dependence of miniband width Δ on ξ for $a = 5.5$ nm; and (c) $\Delta(\xi_m)/\Delta(\xi = 1)$ ratio vs. lattice period a for the $In_{0.53}Ga_{0.47}As/In_{0.52}Al_{0.48}As$ and $GaAs/Al_{0.4}Ga_{0.6}As$ material systems.

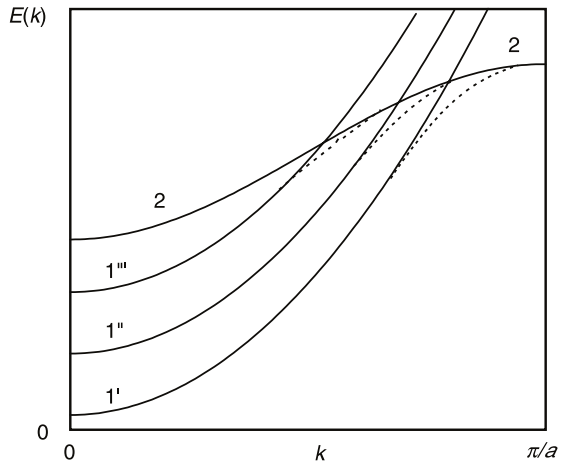

Fig. 4. Hybrid dispersion relation design by channel thickness variation causing a shift in $E_C(0)$ ($1' \rightarrow 1'''$).

The $In_{0.53}Ga_{0.47}As/In_{0.52}Al_{0.48}As$ material system, lattice matched to the InP substrate, has a more favorable δ of 0.51 eV ($m_A = 0.043m_0$, $m_B = 0.072m_0$) than the $GaAs/Al_{0.4}Ga_{0.6}As$ material system. It was also investigated. As shown in Fig. 3(c) for both material systems, $\Delta(\xi_m)/\Delta(1)$ decreases with increasing a almost linearly, which means that $\Delta(\xi_m)$ decreases much faster than $\Delta(\pm 1)$. It also remains below 0.5 over a wide range of SL periods a. The choice of a is a compromise: Narrowing $\Delta(\xi_m)$ by an increase in a_B simplifies the problem of obtaining a hybrid dispersion relation with k_{NEM} far away from π/a, but, in turn, reduces the value of E_{NEM}, which needs to be maximized.

Once the materials for D and C as well as the SL A–B are chosen, and a as well as ξ_m are fixed ($\xi_m \approx -0.25$ for the above $GaAs/Al_{0.4}Ga_{0.6}As$ SL), only the channel thickness a_C remains as a parameter of choice. It allows a relative shift in energy levels of the initial dispersion relations 1 and 2 as schematically shown in Fig. 4. As a result, the intersection point changes and can be placed at a more favorable value of $k_{NEM} < \pi/a$. This optimum channel thickness a_{Co} leads to values of $E_{NEM} - E_C(0)$ that can allow device operation above cryogenic temperatures.

The effective mass actually changes its sign at $k < k_{NEM}$. The critical value k_{NEM}, however, is determined by the tangent at k_{NEM} and the $E_C(0)$ intercept. This point $E_{NEM} = E(k_{NEM})$ corresponds to the onset of current saturation in the I–V characteristics and the formation of a quasi-neutral region in a ballistic n^+nn^+ device, where the ballistic electron plasma is unstable. This instability leads to current oscillations in such a device. However, if the electron transport in the n^+nn^+ device is dissipative, the criteria of instability and oscillations are affected and the critical value of k can differ from k_{NEM}.

Fig. 5 shows the dispersion relations as calculated for two implementations of the proposed nanostructure. In Fig. 5a, results are shown for the $GaAs/Al_{0.4}Ga_{0.6}As$ material system. The calculations assumed that Ψ is not confined to the depletion region within the SL by the electric field of the p–n junction, but by the rather artificial boundary condition $\Psi = 0$ along the z-axis in the SL A–B at $d = 33$ nm from channel C. The SL affects the dispersion relation significantly only if C is thinner than the SL spacing, e.g., $a_C = 4$, 3, and 2 nm, and only if k is near π/a.

In Fig. 5b, the results are shown for the InGaAs/InAlAs material system. Different compositions for A and C as well as B and D are assumed as described in the following. The strained $In_{0.69}Ga_{0.31}As/In_{0.36}Al_{0.64}As$ material system for the SL offers a much more favorable δ of approximately 1.00 eV (as estimated from data in Ref. [13] and with lattice constants of 0.594 and 0.580 nm, respectively) when compared with $\delta = 0.51$ eV for the $In_{0.53}Ga_{0.47}As/In_{0.52}Al_{0.48}As$ material system lattice-matched to the InP substrate. Layer compositions as well as thicknesses a_A and a_B are chosen such that tensile forces in the $In_{0.36}Al_{0.64}As$ layer are compensated by compressive forces in the $In_{0.69}Ga_{0.31}As$ layer and no forces are transferred beyond these two layers. At a period a below the critical value, the lattice mismatch is accommodated elastically and defects or dislocations causing unwanted carrier scattering are avoided. $In_{0.53}Ga_{0.47}As$ is chosen for C and $In_{0.52}Al_{0.48}As$ for D, both lattice-matched to the InP substrate. The energy minimum in the $In_{0.36}Al_{0.64}As$ layer A is 0.18 eV lower than that in the $In_{0.53}Ga_{0.47}As$ channel C. In this system of four materials, a_C controls the shape of the dispersion relations as well as the position of k_{NEM} and E_{NEM} along these curves more effectively and more favorably than in the GaAs/AlGaAs material system of Fig. 5a. In addition, a higher $E_{NEM} - E(0)$ of around 0.15 eV for better RF power generation can be achieved. The best

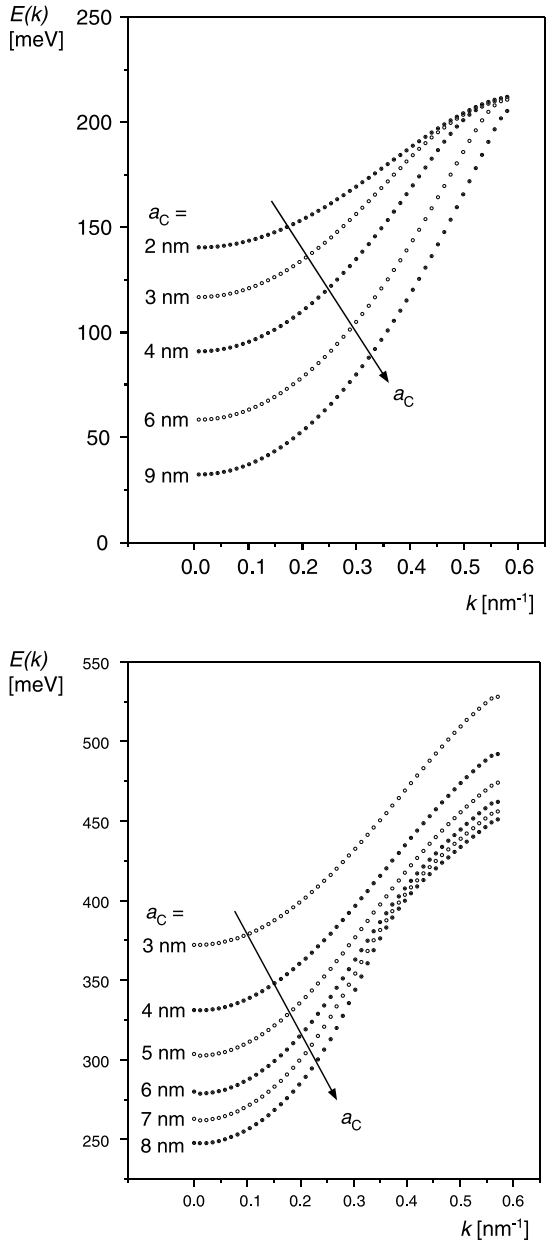

Fig. 5. Hybrid dispersion relations for (a) the GaAs/$Al_{0.4}Ga_{0.6}As$ material system with $a = 5.5$ nm, $a_A = 2.5$ nm, $a_B = 3$ nm, $d = 33$ nm, and different values for a_C; (b) the strained In-GaAs/InAlAs material system with strain compensation, $a_A = 2.5$ nm, $a_B = 3$ nm, $d = 3a_C$, and different values for a_C.

results in this case are obtained for a_C of 6–8 nm, which now exceeds the SL period a of 5.5 nm.

3. Conclusion

Design principles for NEM systems on the basis of a structure with two parallel channels of current conduction were investigated. One channel uses a SL as a region of high effective electron mass. These principles were illustrated by examples from different material systems. More favorable results than in the GaAs/AlGaAs material system can be obtained with structures using strained InGaAs/InAlAs layers with strain compensation and $\delta \geqslant 1.00$ eV.

Acknowledgements

This work was supported by AFOSR through the MURI program (F49620-00-1-0328) and by NSF (ECS-9813823 and ECS-0099913).

References

[1] R.R. Bashirov, Z.S. Gribnikov, N.Z. Vagidov, V.V. Mitin, Appl. Phys. Lett. 77 (2000) 3785.
[2] J.C. Cao, H.C. Liu, X.L. Lei, J. Appl. Phys. 87 (2000) 2867.
[3] J.C. Cao, X.L. Lei, A.Z. Li, H.C. Liu, Appl. Phys. Lett. 78 (2001) 2524.
[4] H. Sakaki, Jpn. J. Appl. Phys. 19 (1980) L735.
[5] P.M. Petroff, A.C. Gossard, R.A. Logan, W. Wigmann, Appl. Phys. Lett. 41 (1982) 635.
[6] L. Pfeiffer, K.W. West, H.L. Stormer, J.P. Eisenstein, K.W. Baldwin, D. Gershoni, J. Spector, Appl. Phys. Lett. 56 (1990) 1697.
[7] T. Fukui, S. Ando, Electron. Lett. 25 (1989) 410.
[8] Y. Nakamura, S. Koshiba, M. Tsuchiya, H. Kano, H. Sakaki, Appl. Phys. Lett. 59 (1991) 700.
[9] S. Shimomura, K. Ohta, Y. Tatsuoka, S. Hiyamizu, K. Fujita, N. Egami, J. Vac. Sci. Technol. B 17 (1999) 1127.
[10] L. Pfeiffer, H.L. Stormer, K.W. Baldwin, K.W. West, A.R. Goni, A. Pinczuk, R.C. Ashori, M.M. Dignam, W. Wegscheider, J. Cryst. Growth 127 (1993) 849.
[11] H. Akiyama, J. Phys.: Condens. Matter 10 (1998) 3095.
[12] W. Wegscheider, G. Schedelbeck, M. Bishler, G. Abstreiter, Physica E 3 (1998) 103.
[13] S. Tiwari, D.J. Frank, Appl. Phys. Lett. 60 (1992) 630.